TISSUE ENGINEERING: Part B
Volume 22, Number 4, 2016

DOI: 10.1089/ten.teb.2015.0453

termis
Tissue Engineering
& Regenerative Medicine
International Society

REVIEW ARTICLE

Ultrasound Imaging Techniques for Spatiotemporal Characterization of Composition, Microstructure, and Mechanical Properties in Tissue Engineering

Cheri X. Deng, PhD, Xiaowei Hong, BS, MS, and Jan P. Stegemann, PhD

Ultrasound techniques are increasingly being used to quantitatively characterize both native and engineered tissues. This review provides an overview and selected examples of the main techniques used in these applications. Grayscale imaging has been used to characterize extracellular matrix deposition, and quantitative ultrasound imaging based on the integrated backscatter coefficient has been applied to estimating cell concentrations and matrix morphology in tissue engineering. Spectral analysis has been employed to characterize the concentration and spatial distribution of mineral particles in a construct, as well as to monitor mineral deposition by cells over time. Ultrasound techniques have also been used to measure the mechanical properties of native and engineered tissues. Conventional ultrasound elasticity imaging and acoustic radiation force imaging have been applied to detect regions of altered stiffness within tissues. Sonorheometry and monitoring of steady-state excitation and recovery have been used to characterize viscoelastic properties of tissue using a single transducer to both deform and image the sample. Dual-mode ultrasound elastography uses separate ultrasound transducers to produce a more potent deformation force to microscale characterization of viscoelasticity of hydrogel constructs. These ultrasound-based techniques have high potential to impact the field of tissue engineering as they are further developed and their range of applications expands.

Introduction

The field of tissue engineering has advanced to the point where the first commercial products are available[1,2] and there is a clear need for nondestructive methods to monitor their development and ensure their quality.[3,4] The ability to reliably characterize engineered tissue constructs in terms of their composition, microstructure, and mechanical properties would greatly facilitate their path to the clinic, and would enable new research directions. In particular, there is a need for techniques that can nondestructively assess key features of engineered tissues in three-dimensional (3D) space and over time.

Ultrasound imaging is the most widely used imaging modality in diagnostic radiology, and its applications are continually being expanded as technology advances. Ultrasound techniques are noninvasive and nondestructive and have proven utility in diagnosis and therapy. In addition, these techniques are relatively cost effective, portable, and translatable between *in vitro* and *in vivo* applications. Therefore, ultrasound techniques are well suited to contribute to the field of tissue engineering by providing an alternative characterization method that can work in conjunction with the existing methods, but also provides new information. In this review, we first examine ultrasound imaging techniques for characterization of the composition and structure of native and engineered tissues. We then focus our attention on ultrasound techniques that have been specifically developed for assessment of mechanical properties in soft tissues and hydrogel scaffolds.

Ultrasound Imaging for Tissue Engineering

Ultrasound imaging typically operates in pulse-echo mode, in which a transducer sends an ultrasound pulse and then receives the backscattered echo signals from the sample under examination. At a fixed location, the time domain echo (A-line) signals provide the locations of acoustic scatterers along the line of sight of the ultrasound pulse, as the signal arrival time from a scatterer is proportional to its distance from the transducer. The amplitudes of the echo signals generally represent the strength of the scatterers, which is related to the local acoustic properties. A two-dimensional (2D) cross-sectional image, or grayscale B-mode image, is

Department of Biomedical Engineering, University of Michigan, Ann Arbor, Michigan.

formed from a collection of A-lines from consecutive locations across a region. A 3D volumetric image can be generated by stacking a set of adjacent 2D images.

The ability of ultrasound to penetrate a wide range of different tissue types and materials makes this technique suitable for noninvasive visualization of the bulk phase of engineered tissues. It is, therefore, a logical extension to exploit the desirable features of ultrasound imaging in tissue engineering applications. Significant progress has been made in this arena. Below, we provide an overview of advanced ultrasound imaging techniques and their applications in tissue engineering.

Grayscale ultrasound imaging for assessment of engineered tissues

Table 1 shows a compilation of representative studies that have employed conventional B-mode ultrasound imaging techniques in tissue engineering applications. A number of pioneering studies used conventional grayscale ultrasound for nondestructive characterization of tissue components and properties in a variety of systems. For example, attenuation of B-mode ultrasound image intensity over time has been shown to correlate with extracellular matrix (ECM) deposition and differentiation of stem cells on 3D synthetic polymer scaffolds.[5] Similarly, grayscale ultrasound imaging has been used to track collagen production by myofibroblasts in 3D fibrin matrices over an 18-day culture time,[6] and to characterize cell number in ceramic composites.[7] In addition, acoustic imaging parameters that represent bulk material properties have even been used to assess matrix evolution by chondrocytes in hydrogels over time.[8,9]

While conventional B-mode ultrasound imaging can provide spatial and temporal information about sample morphology based purely on grayscale values,[10] this approach provides little direct information about sample composition. In addition, purely grayscale signal-based analysis is both system and operator dependent. The imaging signals are affected by a variety of factors not associated with sample properties. These factors include power level of the input signals, ultrasound transducer response, receiver gain, and imaging/signal algorithms for pre- and post-processing and display. Therefore, it is difficult to meaningfully compare the results obtained between ultrasound imaging data taken from different systems or at different times by different operators.[11,12]

Quantitative ultrasound imaging for microscale assessment of engineered tissues

Although any ultrasound-based methods, even those based on conventional B-mode imaging that provide quantitative assessments, may be referred as quantitative ultrasound (QUS) techniques, and in this study, we specifically refer to only those techniques that derive objective, microscopic information related to local tissue composition, and structural details as QUS imaging techniques. QUS imaging techniques are based on the fact that ultrasound propagation and acoustic scattering in tissue or body of the material depends on the local variation of acoustic properties, which in turn is related to tissue microstructure, composition, and other physical properties such as density and compressibility. However, quantitative details of tissue composition are not explicitly apparent from the backscattered signals. Therefore, QUS imaging techniques typically utilize the raw radiofrequency (RF) data of ultrasound backscattered signals to extract objective, quantitative, microscale metrics of tissues. As shown in Table 2, a number of parameters have been exploited as quantitative estimates of the density, size, and spatial organization of acoustic scatterers in the tissue. An important advantage of using raw RF data is the ability to derive results independent of system and operator settings, thereby providing a more objective view of sample characteristics.

QUS imaging has been applied to a broad range of tissue characterization applications (Table 2), for example, to identify changes in tissue state in prostate, breast, and other cancers,[13–15] as well as intravascular plaques.[16] It has also been implemented for monitoring cell death,[17,18] and assessing therapeutic responses in diseased tissues.[19–21] These successful applications have motivated the exploration of QUS approaches in tissue engineering. In the following sections, we discuss two main QUS techniques—use of the integrated backscatter coefficient (IBC) and spectrum analysis—and their application to characterization of engineered tissues.

The IBC for tissue characterization. The IBC has been used as a QUS parameter for tissue characterization.[22] The IBC is an estimate of the backscattered intensity of the subresolution scatterers per unit volume of tissue under examination over the transducer bandwidth.[23] Although the scatterers are too small to be resolved individually in ultrasound imaging,

Table 1. Representative Studies Employing B-Mode Ultrasound Imaging for Tissue Engineering Applications

Representative studies	*Imaging parameters*	*Imaging frequency, MHz*	*References*
Evaluation of extracellular matrix deposition and differentiation of stem cells on 3D synthetic polymer scaffolds	Attenuation	40 focused	Fite *et al.*[5]
Tracking of collagen production by myofibroblasts in 3D fibrin matrices over an 18 day culture time	Grayscale ultrasound imaging	13 linear array	Kreitz *et al.*[6]
Characterization of cell number in ceramic composites	Ultrasound amplitude	N/A	Oe *et al.*[7]
Monitoring of cartilaginous matrix evolution in degradable PEG hydrogels	Speed of sound, slope of attenuation	50 and 100	Rice *et al.*[8]
Evaluation of agarose hydrogel mechanical properties	Speed of sound	15	Walker *et al.*[9]

3D, three-dimensional; PEG, poly(ethylene glycol); N/A, not applicable.

Table 2. Representative Studies Employing Quantitative Ultrasound Imaging Techniques for Tissue Engineering Applications

Representative studies	*Imaging parameters*	*Imaging frequency, MHz*	*References*
Estimation of cell concentration in 3D agarose constructs	Integrated backscatter coefficient	30 and 38	Mercado *et al.*[24]
Assessment of spatial variation in collagen fiber density and diameter in 3D hydrogels	Integrated backscatter coefficient	38	Mercado *et al.*[25]
Spatiotemporal characterization of mineralization in 3D collagen hydrogels	Midband fit and slope	55	Gudur *et al.*[37]
Quantification of osteoblast differentiation in 3D collagen hydrogels	Midband fit, slope, scatterer size, equivalent number of scatterers, relative acoustic impedance	55	Gudur *et al.*[38]

which typically uses frequencies in the MHz range, the IBC provides a quantitative metric that approximates the scatterer number density.[20,23] The IBC method can, therefore, be used to estimate the cell density and spatial distribution in tissue constructs. In a recent study by Mercado *et al.*,[24] the IBC, calculated from the measured backscattered RF data in a frequency range of 13–47 MHz, was used to noninvasively estimate cell concentration in agarose gels. It was found that the IBC for cell-seeded gels increased linearly as cell density increased, suggesting that IBC values may represent the collective strength of the cells serving as acoustic scatterers in the constructs. It was also shown that both the accuracy and precision of IBC estimation improved with increasing region of interest (ROI) dimensions and cell concentration. These results are promising, and were obtained completely nondestructively. While this study examined only one time point, it served as proof of concept that the IBC could be used to monitor cell populations within engineered tissue constructs.

The IBC method has also been extended to characterize collagen-based biomaterials,[25] which are widely investigated as scaffolds in tissue engineering. As with cellular characterization, noninvasive techniques capable of visualizing collagen fiber microstructure would greatly aid the development of functional engineered tissues. In acellular collagen gels, the IBC increased linearly with increasing collagen concentration, indicating that collagen can act as an effective acoustic scatterer in such constructs. In contrast, collagen gels fabricated at a higher polymerization temperature exhibited lower IBC values. Interestingly, IBC parametric images allowed visualization of the spatial variation in collagen distribution caused by the geometry of the gels studied, as shown in Figure 1. This work demonstrated that IBC analysis can be used to indirectly examine the microstructure and spatial composition of 3D collagen matrices even in the absence of stronger scatterers such as cells.

Spectrum analysis for tissue characterization. Frequency domain analysis of backscattered RF signals in ultrasound imaging has also been exploited to provide objective, quantitative tissue characterization.[10,11,26,27] In this approach, power spectra of the RF signals from an ROI are computed and calibrated so that the system effects are removed. Instead of obtaining an aggregate parameter such as

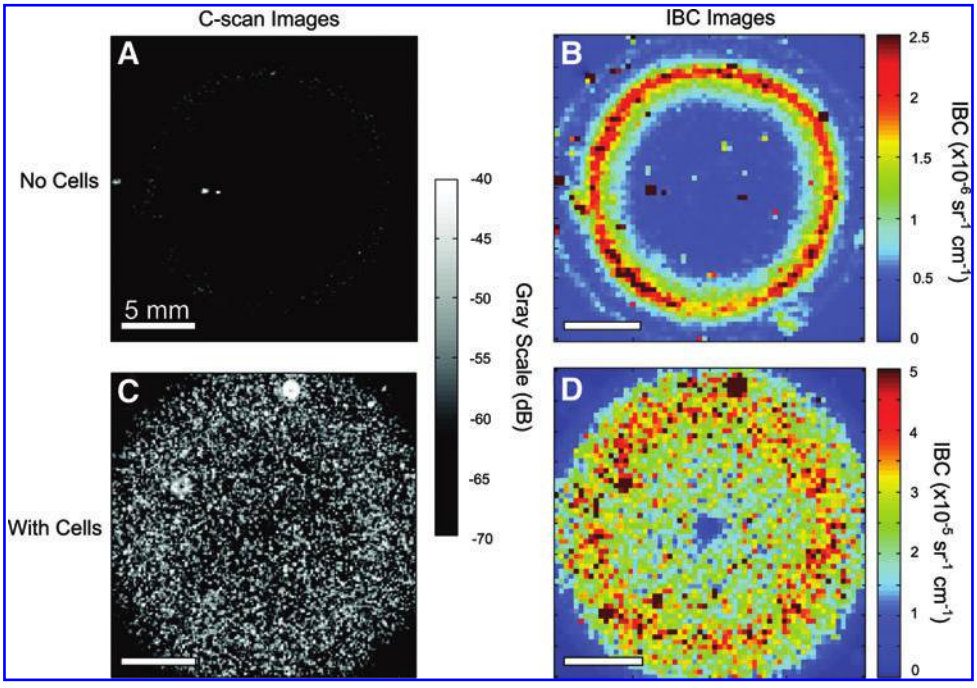

FIG. 1. **(A, B)** C-scan and integrated backscatter coefficient (IBC) parametric imaging of acellular and **(C, D)** cell-seeded collagen gels. Best viewed in *color*. Adapted from Mercado *et al.*[25] and used with permission. Color images available online at www.liebertpub.com/teb

the integrated IBC, spectrum analysis generates spectral parameters that can provide additional information about the underlying tissue microstructure. The spectrum analysis technique has been used in various applications, including characterization of plaque composition by intravascular ultrasound,[16,28,29] and lesions induced by high-intensity focused ultrasound.[30,31] Spectral parameters have also shown the ability to identify changes in a tissue state for a number of organ systems, including the prostate, pancreas, and lymph node.[15,32,33]

The technique is based on the fact that spectral characteristics of the backscattered RF data include information of the effective acoustic scatterers in the tissue. As these scatterers are generally much smaller compared with the ultrasound wavelength, the calibrated spectra of the RF data are often quasilinear over the bandwidth used in typical ultrasound imaging. Therefore, a linear regression is sufficient to obtain a set of parameters from the calibrated tissue spectra. The parameters typically used include the slope and intercept of the regression line, as well as the midband fit (MBF), which is the value of the regression line at the midpoint of the usable bandwidth used in the spectral analysis. Importantly, it has been shown theoretically that these spectral regression parameters are related to tissue microstructural properties.[12,26,34] For example, spectral slope depends on the scatterer size, whereas MBF relates to size, concentration, and relative acoustic impedances of the scattering elements.[26]

Spectrum analysis can be applied to data from conventional ultrasound imaging (5–15 MHz) in diagnostic radiology,[35] as well as to high-frequency ultrasound imaging (20–60 MHz). The advantage of high frequencies, with wavelengths on the order of 100 μm, is that the higher resolution allows characterization of smaller tissue structures. Spectral analysis has been implemented to characterize the properties of cell aggregates that were used as simplified models of tumors.[17,35] and it was possible to detect cellular changes after exposure to chemotherapy.[36] In particular, it was found that ultrasound backscatter intensity and spectral slope increased after treatment, due to the decrease in the effective scatterer size associated with changes in cell nuclei and cell structure.

We recently implemented a high-frequency spectral ultrasound imaging (SUSI) technique for noninvasive, quantitative assessment of engineered tissues. SUSI was applied to a model construct that mimics developing mineralized tissue.[37] Figure 2 shows a schematic of the SUSI setup used. The SUSI technique was validated using collagen hydrogels doped with known amounts of hydroxyapatite mineral (HA). Example grayscale and parametric images of HA-doped collagen gels are presented in Figure 3. It was shown that the MBF corresponded to HA concentration and, therefore, could be used to characterize the distribution of particles in the constructs. The spectral slope was inversely related to HA particle size and, therefore, could be used to discriminate between different grades of HA. Exogenous mineralization of collagen gels was also induced through incubation in a high ionic strength solution to assess the ability of SUSI to monitor changes in the constructs over time, and to correlate spectral parameters with the concentration of mineral in the constructs. Figure 4 shows example grayscale and parametric images at two time points. The MBF was useful in showing the pattern of mineral precipitation and the densification of the constructs over time. The slope parameter showed how particle size increased over time as mineral accretion progressed.

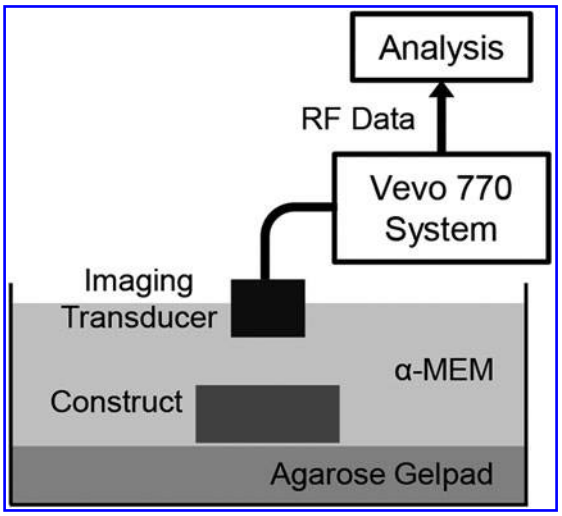

FIG. 2. Schematic of experimental setup used for spectral ultrasound imaging (SUSI) of tissue construct. Adapted from Gudur *et al.*[37] and used with permission.

In a follow-up study, we applied high-resolution SUSI to quantitatively characterize the differentiation of preosteoblast cells seeded in 3D collagen-based engineered tissues.[38] SUSI was used to assess the compositional features of the cell-seeded constructs, including cell size, cell number, and calcium deposition. Estimation of cell size using the spectral slope parameter resulted in a value of 12–15 μm, which is larger than the nucleus alone and suggests that the cell body may also be involved in the scattering of ultrasound. Cell numbers were estimated based on the acoustic concentration (CQ^2) per unit volume, and agreed well with values obtained by conventional biochemical analysis at early time points. However, as the cells in the constructs differentiated, the cell number estimates became less accurate, presumably due to increased acoustic impedance caused by cellular calcium deposition. The value of the relative acoustic impedance was also used to estimate the mass of calcium deposited, which matched closely with data obtained by destructive biochemical analysis. Taken together, these studies have shown how QUS techniques can be applied to examine the spatial variation and temporal evolution of the composition and structure of engineered tissues.

Ultrasound Techniques for Assessment of Mechanical Properties

While grayscale B-mode ultrasound imaging is useful to understand tissue morphology and QUS imaging can assess certain aspects of tissue composition and microstructure, ultrasound imaging techniques also have potential for characterizing the mechanical properties of native and engineered tissues.[39,40] For example, ultrasound elastography techniques are based on the fact that ultrasound can detect signal changes that are specifically associated with the mechanical properties of tissue such as the stiffness or Young's modulus. Measurement of the speed of sound within a sample has also been used to characterize hydrogel mechanical properties.[9] Chung *et al.*[41] recently reported a study

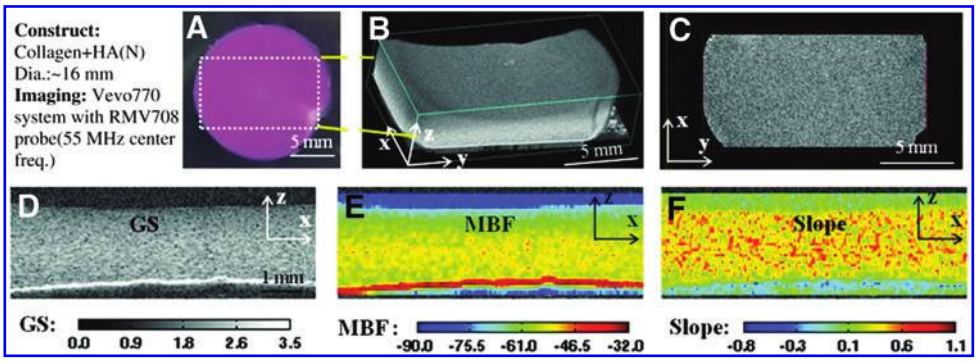

FIG. 3. Virtual histology of three-dimensional (3D) collagen construct with added hydroxyapatite mineral. **(A)** Color image of the top view of constructs. **(B)** 3D ultrasound rendered image of the region outlined in **(A)**. **(C)** Ultrasound C-scan of a transverse *x*–*y* plane. **(D)** Grayscale (GS), **(E)** midband fit (MBF), and **(F)** slope parametric images of one section in the *x*–*z* plane. Best viewed in *color*. Adapted from Gudur *et al.*[37] and used with permission. Color images available online at www.liebertpub.com/teb

that estimated regional strains using ultrasound pulse-echo detection of a displacement generated by indentation of multilayered hydrogels and tissue-engineered cartilage. Excellent reviews of ultrasound elasticity imaging (UEI) methods have been provided by Greenleaf *et al.,*[42] Parker *et al.,*[43] Palmeri and Nightingale,[44] and DeWall.[42] In the subsections below, we first summarize two main forms of ultrasound elastography: conventional UEI and acoustic radiation force (ARF) elasticity imaging. We then focus our attention to ultrasound techniques for assessing viscoelasticity for tissue engineering applications.

Ultrasound techniques for quantification of tissue stiffness

UEI,[45,46] also called ultrasound elastography, has been exploited for tumor detection and other applications in which detection of spatial variation of tissue stiffness is informative.[45,47,48] These techniques are based on the differences of tissue displacements in uncompressed versus compressed tissues, as determined by ultrasound echo signals. Kim *et al.* have reported the use of ultrasound strain imaging technique for noninvasive monitoring of tissue scaffold degradation in tissue engineering.[49]

In conventional UEI, an external static load is applied to the surface of a tissue to generate compression, usually through a mechanical device such as a platen. A sequence of pre- and postcompression ultrasound images are processed using a cross-correlation algorithm or speckle tracking scheme to detect the displacement at each location within the sample, to infer the elasticity inside the sample.[50,51] This technique has a particular advantage in imaging the spatial variation of mechanical properties within a tissue volume. For example, if a soft or hard inclusion is present in the tissue sample, the relative local deformation will exhibit a pattern that depends on the size of the inclusion and its stiffness relative to the surrounding material. UEI techniques exploit the same idea as manual palpation, but provide images of tissue volume with richer information in a more systematic and controlled fashion.

ARF elasticity imaging uses the force associated with an ultrasound beam as a means to achieve deformation in a material body in a noncontact fashion.[40] Unlike the conventional form of UEI, ARF is a body force generated within a material sample generated by momentum transfer from the ultrasound wave to the medium.[40] For a plane wave, the ARF is proportional to the acoustic intensity, which is the time average of the acoustic pressure. If it is of sufficient magnitude, such a force may be used to induce tissue compression. In conventional ultrasound imaging, the ARF associated with the imaging pulse is small so that tissue deformation is negligible. However, an elegant form of ARF elasticity imaging, called acoustic radiation force impulse (ARFI)[52,53] imaging adjusts the pulse intensity on selected pulses and, therefore, can use the same pulse-echo ultrasound imaging system to generate both the compression

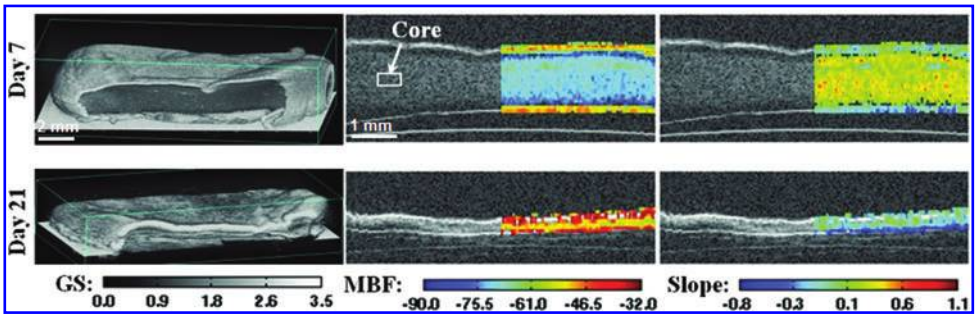

FIG. 4. 3D rendered (*first column*), MBF superimposed on GS (*second column*), and slope superimposed on GS (*third column*) images of collagen constructs mineralized in simulated body fluid on day 7 and day 21. Best viewed in *color*. Adapted from Gudur *et al.*[37] and used with permission. Color images available online at www.liebertpub.com/teb

ultrasound pulses, as well as the imaging pulses for detecting tissue displacements. Figure 5 shows example grayscale and ARFI images for live tissue during a RF ablation procedure.[54]

Ultrasound techniques for quantification of viscoelastic properties

In general, soft tissues are viscoelastic, inhomogeneous, and anisotropic,[55] exhibiting properties of both elastic solids and viscous fluids. Engineered tissues typically make use of cells and biomaterial scaffolds that mimic key properties of the ECM, including biomechanical properties. Therefore, assessment of the material properties is an important tool in developing engineered tissues. However, current mechanical characterization methods are limited by the need for contact with the sample and their inherently destructive nature, which make them difficult to apply to cellular engineered constructs. Ultrasound techniques offer a new way of characterizing engineered tissues, particularly those based on hydrogel scaffolds, which typically display viscoelastic properties.

Sonorheometry and monitoring of excitation and recovery using ARF imaging. Sonorheometry uses a series of high pulse repetition frequency (PRF) pulses to effectively generate a step excitation of a desired duration in the sample.[56] This approach provides extended deformation and permits the measurement of the viscoelastic properties of a material. Walker *et al.*[57] used this technique with a 10 MHz transducer to obtain the time–displacement curve from a sample. By fitting the time–displacement curve with a Voigt model, the relative elasticity and viscosity of the samples were derived. Since the ARF associated with typical imaging pulses are very small, Mauldin *et el.* extended the approach to allow monitoring of steady-state excitation and recovery (MSSER) of deformation in a sample before and after a step-stress application.[58] Similar to ARFI elastography, the MSSER technique used two types of pulses using the same imaging system for both imaging and pushing, with 6.15 and 4.21 MHz center frequency, respectively. The pushing pulses were generated simply by increasing the acoustic pressure amplitude of the ultrasound pulses to deform the tissue more efficiently.

The sonorheometry and MSSER techniques employ the same ultrasound transducer and system for ARF application and imaging. While this configuration has advantages, it can also be restricting due to contradicting requirements for the compressing and imaging ultrasound beams. For example, high frequency is preferred to achieve high axial resolution for imaging. However, the correspondingly higher attenuation at high frequency results in reduced penetration depth. In addition, axial energy distribution at high frequency creates an inhomogeneous force field, complicating the analysis required to map the spatial distribution of viscoelastic properties. Also, these approaches require protocols to generate ARF pushing pulses with increased intensity, which may present a technical barrier for working with commercial systems. Finally, while adjusting acoustic pressure amplitude and duration of the ultrasound pulses

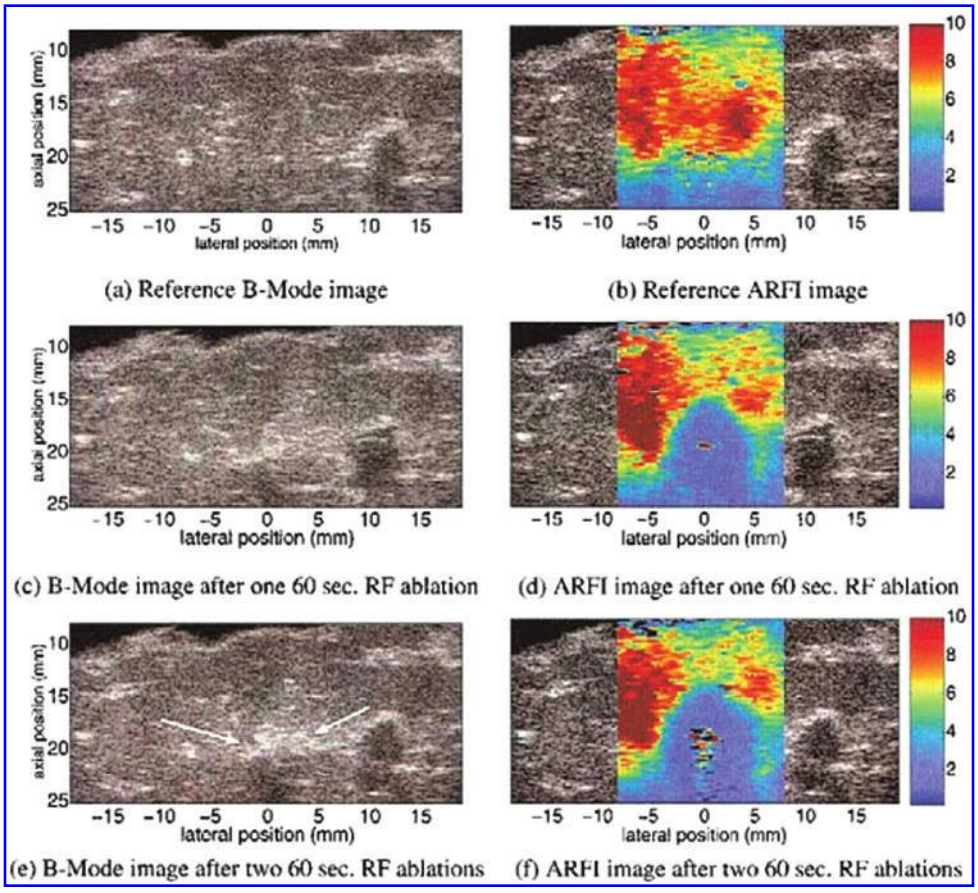

FIG. 5. B-mode and acoustic radiation force impulse (ARFI) images of liver sample before **(a** and **b)** and after **(c** to **f)** radiofrequency (RF) ablation procedure. Best viewed in *color*. Adapted from Fahey *et al.*[54] and used with permission. Color images available online at www.liebertpub.com/teb

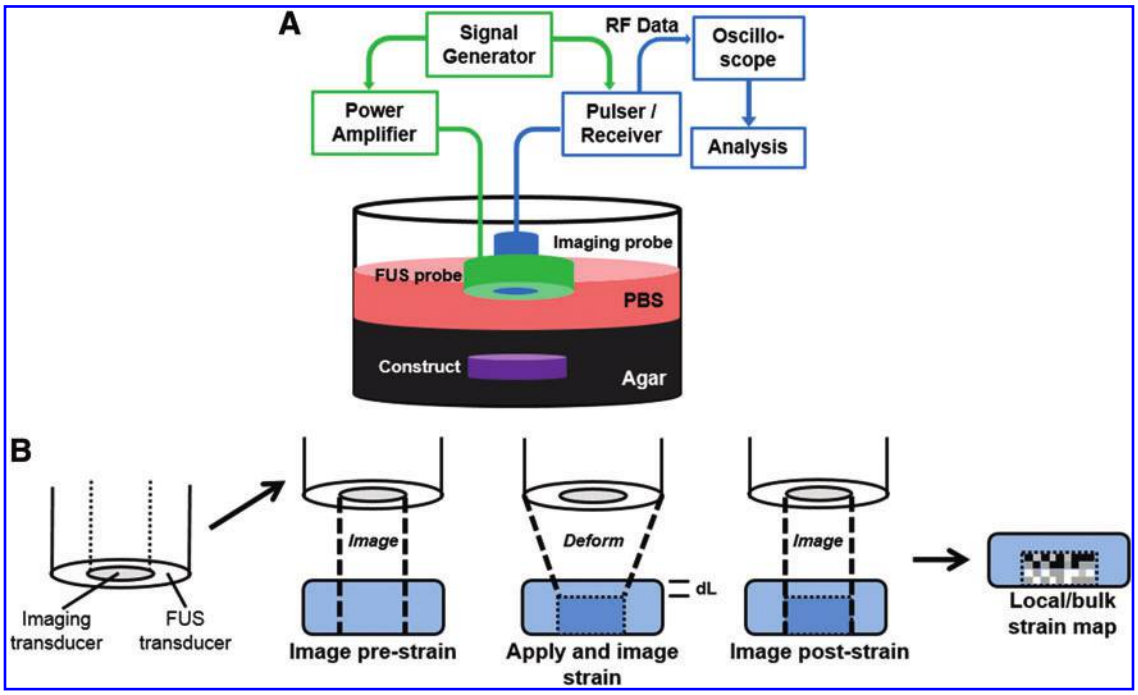

FIG. 6. **(A)** Schematic of experimental setup used for dual-mode ultrasound elastography (DUE) of hydrogel constructs, and **(B)** principle of dual-mode deformation and imaging. Color images available online at www.liebertpub.com/teb

that may be achieved with the same transducer, it may be difficult to alter the spatial beam characteristics using the same transducer.

Dual-mode ultrasound elastography for quantification of viscoelastic properties. We have developed a dual-mode ultrasound elastography (DUE) approach that uses focused ultrasound (FUS, 2 MHz center frequency) pulses to induce compression in a sample, and a separate ultrasound imaging system (10 MHz) to detect the deformation within the sample. The use of a stand-alone compression transducer allows flexibility in specifying the beam profile, acoustic pressure amplitude, and pulse duration most suitable for providing sufficient compression to specific materials, and for interleaving with the ultrasound imaging component. This set-up allows the frequency of the ultrasound imaging system to be selected to provide the needed spatial resolution and penetration depth for specific applications. Figure 6 shows a schematic of a DUE set-up for *in vitro* testing (Fig. 6A), as well as a schematic of the technique used to generate both a compression force and imaging data (Fig. 6B). FUS pulses are produced by the outer annular transducer to compress the sample using an appropriate PRF, for example, 1 Hz and 99% duty cycle. Pulses from the inner imaging transducer are interleaved to allow acquisition of echo signals during the off periods of the FUS pulses. The pulse scheme of FUS and imaging probes enables monitoring of construct deformation before, during, and after compression, from which creep and recovery responses are obtained.

Quantitative DUE can be applied to determine the viscoelastic properties of biomaterials. Analysis of an A-line signal acquired as a function of time provides the time-dependent M-mode data,[59] and this analysis is readily applied to a collection of A-line signals for a 2D B-mode or 3D operation. M-mode images, therefore, illustrate the changes in RF signals at different depths in the sample as a function of time. Local displacement of a material at a spatial location due to FUS compression can be determined from the temporal shift of the RF signal at the location, compared to precompression.[60] The spatiotemporal distribution of tissue displacement can be then calculated to produce a displacement map. From the displacement data, strain as a function of time at a given location can then be calculated by analyzing a small segment along the A-line at the desired location. The change in thickness of the sample or of a selected segment within the sample can be determined using the imaging data, and both bulk and local strains can be calculated from these displacement data.

In an initial study, we applied DUE to 3D collagen hydrogels *in vitro*. Figure 7 shows an example of the resulting bulk strain data and three segment strains as a function of time. The strain data exhibit characteristics typical of viscoelastic materials, including a creep and relaxation phase during and after stress application, respectively. Strain increased with increasing acoustic pressure through FUS application, indicating that higher ARFs were applied to the constructs by FUS with higher acoustic pressures, as expected. Testing of constructs made with different collagen concentrations showed that the same acoustic pressure generated higher strains in the constructs with lower collagen, indicating that higher collagen concentration yielded stiffer constructs. For more comprehensive characterization, we also fit the measured strain data to Burger's model of viscoelastic materials.[61] This model contains elements that represent the elastic and viscous response to strain, as shown in Figure 8A. Fitting of the DUE creep data to the model under constant compressive stress can be used to provide insight into material properties.[62] Figure 8B shows an example of

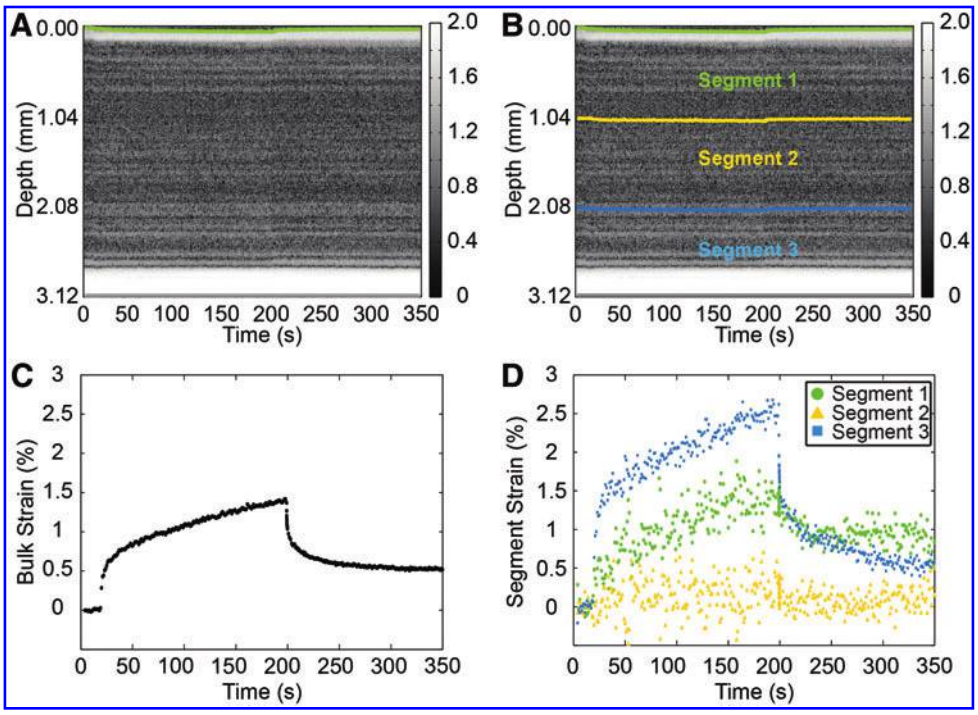

FIG. 7. GS images of fibrin constructs with boundaries outlined for **(A)** the entire construct and **(B)** three internal segments. **(C)** Bulk strain–time curve. **(D)** Strain–time curve for three segments. Color images available online at www.liebertpub.com/teb

parameters derived from model fitting for HA-doped agarose hydrogels and cellular collagen constructs.

The DUE technique is notable because of the way strain is applied to and detected in the sample. In conventional mechanical testing, deformation is generated by physical compression or stretch applied to a boundary of a sample.[63,64] As the sample is deformed, strain is generated through the molecular forces within the material. Bulk properties such as Young's modulus are calculated based on the relationship between the overall (bulk) stress and strain values. However, this approach provides no information on local strains or on the spatial variation of properties within the material. In contrast, DUE applies stress through the ARF associated with a FUS beam. The ARF is a body force whose spatial distribution is determined by the ultrasound beam shape and acoustic attenuation of the material. Therefore, the strain distribution within

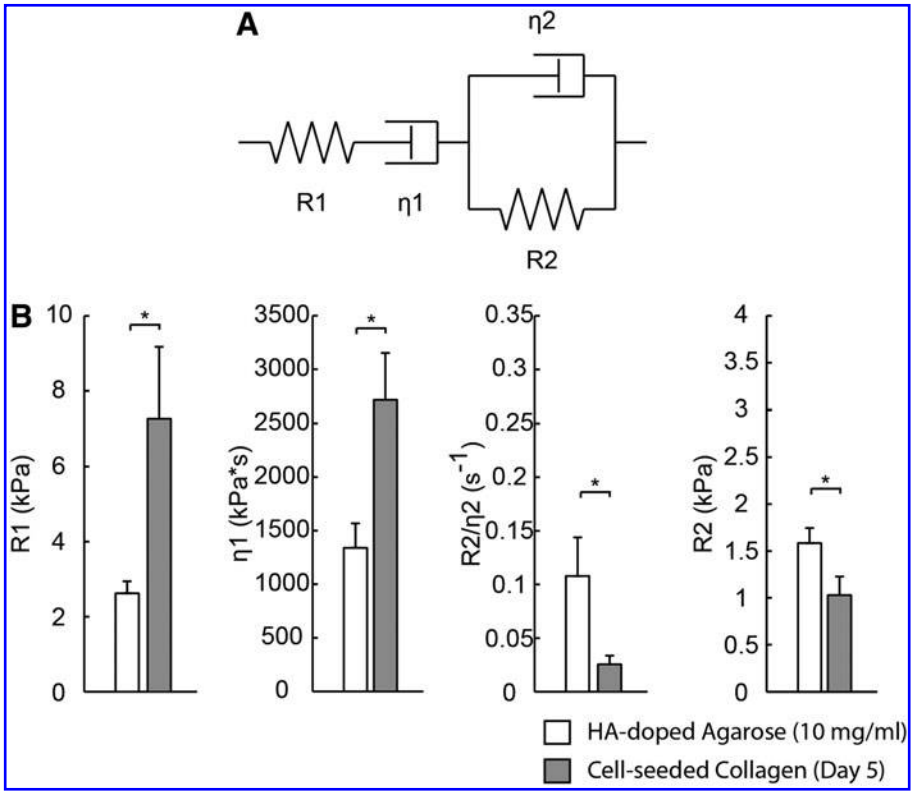

FIG. 8. **(A)** Schematic of four-parameter Burger's viscoelastic model. **(B)** Model parameters obtained from creep curve for hydroxyapatite (HA)-doped agarose constructs and cell-seeded collagen constructs on day 5 ($N=4$).

a material is distinct from that produced by a contact force applied to the sample surface, even if the bulk strain is the same in both cases. For example, if the axial profile of an ARF field is uniform and constant, then the strain generated in a sample will be similar to the force produced by gravity in the vertical direction. If the material is inhomogeneous, which affects the ARF spatial distribution, the ARF-induced strain within the sample will also vary spatially.

Importantly, the strain distribution within a sample can be characterized using DUE. Therefore, this technique provides not only a method to measure the viscoelastic properties of a material, but also a means to investigate and map the spatiotemporal stress–strain response. This capability makes it perhaps uniquely suited to studying aspects of the cellular microenvironment and mechanobiology that cannot be investigated using conventional mechanical testing methods.

Summary and Future Perspectives

Ultrasound techniques have proven their value in a wide range of *in vitro* and *in vivo* tissue characterization applications. These methods are particularly valuable in characterizing the spatial variation of tissue composition and properties, as well as in noninvasively monitoring tissue development over time. The use of nonionizing radiation in ultrasound techniques to provide rapid, noninvasive, and image-based data, therefore, also has great potential in characterizing engineered tissues.

Ultrasound-based methods offer potentially important advantages over other tissue characterization techniques, and *in vitro* applications are progressively being translated to *in vivo* and clinical use. For example, UEI is now an Food and Drug Administration (FDA)-approved technique for diagnostic breast imaging and classifying suspicious lesions.[65] Various forms of UEI techniques have also been exploited for other applications, including characterizing contractility and strain in the myocardium.[66–68] Similarly, ARFI imaging has been investigated for multiple clinical applications, including assessment of changes in cardiac tissue stiffness[69] and detection of tumors in the prostate.[70] A version of ARFI elastography, called Virtual Touch Tissue Imaging, has been implemented on a commercial system with on-going clinical evaluations in Europe and Asia.[40]

An important challenge in translating ARF-based ultrasound elastography techniques to *in vivo* applications is the difficulty in quantitatively characterizing the ARF. Relative measurements of tissue stiffness are useful in differentiating between healthy and diseased tissues. However, in some cases quantification of the material properties is preferred or necessary. *In vitro* characterization of the ARF has been pursued; however, strategies to determine its magnitude *in vivo* are also needed.

Ultrasound is unique in the way it interacts with biological tissue, offering the possibility of generating new kinds of mechanical properties data at scales relevant to cellular mechanobiology. The excellent tissue penetration and wide range of ultrasound frequencies and choice of other operating parameters make ultrasound techniques very versatile. Ultrasound is increasingly being applied to applications in tissue characterization, and offers a way to generate information-rich, quantitative representations of both native and engineered tissues.

Acknowledgments

The authors are grateful to their colleagues in the field for their valuable insight and discussions. The authors have used selected examples of published studies to illustrate strategies for use of ultrasound techniques in tissue engineering, and apologize to those whose work could not be included due to space limitations. This work was supported, in part, by the National Institute of Arthritis and Musculoskeletal and Skin Diseases under award numbers R21AR064041 (to C.X.D. and J.P.S.) and R01AR062636 (to J.P.S.). The content is solely the responsibility of the authors and does not necessarily represent the official views of the National Institutes of Health.

Disclosure Statement

No competing financial interests exist.

References

1. Rice, J.B., Desai, U., Ristovska, L., Cummings, A.K., Birnbaum, H.G., Skornicki, M., Margolis, D.J., and Parsons, N.B. Economic outcomes among medicare patients receiving bioengineered cellular technologies for treatment of diabetic foot ulcers. J Med Econ **18,** 586, 2015.
2. Zaslav, K., Cole, B., Brewster, R., DeBerardino, T., Farr, J., Fowler, P., and Nissen, C.; STAR Study Principal Investigators. A prospective study of autologous chondrocyte implantation in patients with failed prior treatment for articular cartilage defect of the knee: results of the Study of the Treatment of Articular Repair (STAR) clinical trial. Am J Sports Med **37,** 42, 2009.
3. Trachtenberg, J.E., Vo, T.N., and Mikos, A.G. Pre-clinical characterization of tissue engineering constructs for bone and cartilage regeneration. Ann Biomed Eng **43,** 681, 2015.
4. Appel, A.A., Anastasio, M.A., Larson, J.C., and Brey, E.M. Imaging challenges in biomaterials and tissue engineering. Biomaterials **34,** 6615, 2013.
5. Fite, B.Z., Decaris, M., Sun, Y.H., Sun, Y., Lam, A., Ho, C.K.L., Leach, J.K., and Marcu, L. Noninvasive multimodal evaluation of bioengineered cartilage constructs combining time-resolved fluorescence and ultrasound imaging. Tissue Eng Part C Methods **17,** 495, 2011.
6. Kreitz, S., Dohmen, G., Hasken, S., Schmitz-Rode, T., Mela, P., and Jockenhoevel, S. Nondestructive method to evaluate the collagen content of fibrin-based tissue engineered structures via ultrasound. Tissue Eng Part C Methods **17,** 1021, 2011.
7. Oe, K., Miwa, M., Nagamune, K., Sakai, Y., Lee, S.Y., Niikura, T., Iwakura, T., Hasegawa, T., Shibanuma, N., Hata, Y., Kuroda, R., and Kurosaka, M. Nondestructive evaluation of cell numbers in bone marrow stromal cell/beta-tricalcium phosphate composites using ultrasound. Tissue Eng Part C Methods **16,** 347, 2010.
8. Rice, M.A., Waters, K.R., and Anseth, K.S. Ultrasound monitoring of cartilaginous matrix evolution in degradable PEG hydrogels. Acta Biomater **5,** 152, 2009.
9. Walker, J.M., Myers, A.M., Schluchter, M.D., Goldberg, V.M., Caplan, A.I., Berilla, J.A., Mansour, J.M., and Welter, J.F. Nondestructive evaluation of hydrogel mechanical properties using ultrasound. Ann Biomed Eng **39,** 2521, 2011.
10. Insana, M.F., and Brown, D.G. Acoustic scattering theory applied to soft biological tissues. In: Shung K.K., ed. Ultrasonic Scattering in Biological Tissues. Boca Raton: CRC Press, 1993, p. 75.

11. Lizzi, F.L., Greenebaum, M., Feleppa, E.J., Elbaum, M., and Coleman, D.J. Theoretical framework for spectrum analysis in ultrasonic tissue characterization. J Acoust Soc Am **73,** 1366, 1983.
12. Lizzi, F.L., Astor, M., Liu, T., Deng, C., Coleman, D.J., and Silverman, R.H. Ultrasonic spectrum analysis for tissue assays and therapy evaluation. Int J Imaging Syst Technol **8**, 3, 1997.
13. Feleppa, E.J., Ennis, R.D., Schiff, P.B., Wuu, C.S., Kalisz, A., Ketterling, J., Urban, S., Liu, T., Fair, W.R., Porter, C.R., and Gillespie, J.R. Spectrum-analysis and neural networks for imaging to detect and treat prostate cancer. Ultrason Imaging **23,** 135, 2001.
14. Golub, R.M., Parsons, R.E., Sigel, B., Feleppa, E.J., Justin, J., Zaren, H.A., Rorke, M., Sokilmelgar, J., and Kimitsuki, H. Differentiation of breast-tumors by ultrasonic tissue characterization. J Ultrasound Med **12,** 601, 1993.
15. Feleppa, E.J. Ultrasonic tissue-type imaging of the prostate: implications for biopsy and treatment guidance. Cancer Biomark **4**, 201, 2008.
16. Nasu, K., Tsuchikane, E., Katoh, O., Vince, D.G., Virmani, R., Surmely, J.F., Murata, A., Takeda, Y., Ito, T., Ehara, M., Matsubara, T., Terashima, M., and S uzuki, T. Accuracy of in vivo coronary plaque morphology assessment—a validation study of in vivo virtual histology compared with in vitro histopathology. J Am Coll Cardiol **47,** 2405, 2006.
17. Kolios, M.C., Czarnota, G.J., Lee, M., Hunt, J.W., and Sherar, M.D. Ultrasonic spectral parameter characterization of apoptosis. Ultrasound Med Biol **28,** 589, 2002.
18. Brand, S., Weiss, E.C., Lemor, R.M., and Kolios, M.C. High frequency ultrasound tissue characterization and acoustic microscopy of intracellular changes. Ultrasound Med Biol **34,** 1396, 2008.
19. Ghoshal, G., Kemmerer, J.P., Karunakaran, C., Abuhabsah, R., Miller, R.J., Sarwate, S., and Oelze, M.L. Quantitative ultrasound imaging for monitoring in situ high-intensity focused ultrasound exposure. Ultrason Imaging **36,** 239, 2014.
20. Vlad, R.M., Brand, S., Giles, A., Kolios, M.C., and Czarnota, G.J. Quantitative ultrasound characterization of responses to radiotherapy in cancer mouse models. Clin Cancer Res **15,** 2067, 2009.
21. Kemmerer, J.P., and Oelze, M.L. Ultrasonic assessment of thermal therapy in rat liver. Ultrasound Med Biol **38,** 2130, 2012.
22. Thomas, L.J., Barzilai, B., Perez, J.E., Sobel, B.E., Wickline, S.A., and Miller, J.G. Quantitative real-time imaging of myocardium based on ultrasonic integrated backscatter. IEEE Trans Ultrason Ferroelectr Freq Control **36,** 466, 1989.
23. Insana, M.F., and Hall, T.J. Parametric ultrasound imaging from backscatter coefficient measurements: image formation and interpretation. Ultrason Imaging **12,** 245, 1990.
24. Mercado, K.P., Helguera, M., Hocking, D.C., and Dalecki, D. Estimating cell concentration in three-dimensional engineered tissues using high frequency quantitative ultrasound. Ann Biomed Eng **42,** 1292, 2014.
25. Mercado, K.P., Helguera, M., Hocking, D.C., and Dalecki, D. Noninvasive quantitative imaging of collagen mcrostructure in three-dimensional hydrogels using high-frequency ultrasound. Tissue Eng Part C Methods **21,** 671, 2015.
26. Lizzi, F.L., Ostromogilsky, M., Feleppa, E.J., Rorke, M.C., and Yaremko, M.M. Relationship of ultrasonic spectral parameters to features of tissue microstructure. IEEE Trans Ultrason Ferroelectr Freq Control **34,** 319, 1987.
27. Lizzi, F.L., Feleppa, E.J., Alam, S.K., and Deng, C.X. Ultrasonic spectrum analysis for tissue evaluation. Pattern Recognit Lett **24,** 637, 2003.
28. Nair, A., Kuban, B.D., Tuzcu, E.M., Schoenhagen, P., Nissen, S.E., and Vince, D.G. Coronary plaque classification with intravascular ultrasound radiofrequency data analysis. Circulation **106,** 2200, 2002.
29. Qian, J., Maehara, A., Mintz, G.S., Margolis, M.P., Lerman, A., Rogers, J., Banai, S., Kazziha, S., Castellanos, C., Dani, L., Fahy, M., Stone, G.W., and Leon, M.B. Impact of gender and age on in vivo virtual histology-intravascular ultrasound imaging plaque characterization (from the global virtual vistology intravascular ultrasound [VH-IVUS] registry). Am J Cardiol **103,** 1210, 2009.
30. Gudur, M.S., Kumon, R.E., Zhou, Y., and Deng, C.X. High-frequency rapid B-mode ultrasound imaging for real-time monitoring of lesion formation and gas body activity during high-intensity focused ultrasound ablation. IEEE Trans Ultrason Ferroelectr Freq Control **59,** 1687, 2012.
31. Kumon, R.E., Gudur, M.S.R., Zhou, Y., and Deng, C.X. High-frequency ultrasound M-mode imaging for identifying lesion and bubble activity during high-intensity focused ultrasound ablation. Ultrasound Med Biol **38,** 626, 2012.
32. Kumon, R.E., Pollack, M.J., Faulx, A.L., Olowe, K., Farooq, F.T., Chen, V.K., Zhou, Y., Wong, R.C., Isenberg, G.A., Sivak, M.V., Chak, A., and Deng, C.X. In vivo characterization of pancreatic and lymph node tissue by using EUS spectrum analysis: a validation study. Gastrointest Endosc **71,** 53, 2010.
33. Kumon, R.E., Olowe, K., Faulx, A.L., Farooq, F.T., Chen, V.K., Zhou, Y., Wong, R.C., Isenberg, G.A., Sivak, M.V., Chak, A., and Deng, C.X. EUS spectrum analysis for in vivo characterization of pancreatic and lymph node tissue: a pilot study. Gastrointest Endosc **66,** 1096, 2007.
34. Lizzi, F.L., Astor, M., Feleppa, E.J., Shao, M., and Kalisz, A. Statistical framework for ultrasonic spectral parameter imaging. Ultrasound Med Biol **23,** 1371, 1997.
35. Vlad, R.M., Alajez, N.M., Giles, A., Kolios, M.C., and Czarnota, G.J. Quantitative ultrasound characterization of cancer radiotherapy effects in vitro. Int J Radiat Oncol Biol Phys **72,** 1236, 2008.
36. Czarnota, G.J., Kolios, M.C., Abraham, J., Portnoy, M., Ottensmeyer, F.P., Hunt, J.W., and Sherar, M.D. Ultrasound imaging of apoptosis: high-resolution non-invasive monitoring of programmed cell death in vitro, in situ and in vivo. Br J Cancer **81,** 520, 1999.
37. Gudur, M., Rao, R.R., Hsiao, Y.S., Peterson, A.W., Deng, C.X., and Stegemann, J.P. Noninvasive, quantitative, spatiotemporal characterization of mineralization in three-dimensional collagen hydrogels using high-resolution spectral ultrasound imaging. Tissue Eng Part C Methods **18,** 935, 2012.
38. Gudur, M.S., Rao, R.R., Peterson, A.W., Caldwell, D.J., Stegemann, J.P., and Deng, C.X. Noninvasive quantification of in vitro osteoblastic differentiation in 3D engineered tissue constructs using spectral ultrasound imaging. PLoS One **9**, e85749, 2014.
39. Sarvazyan, A., Hall, T.J., Urban, M.W., Fatemi, M., Aglyamov, S.R., and Garra, B.S. An overview of elastography—an emerging branch of medical imaging. Curr Med Imaging Rev **7**, 255, 2011.
40. Doherty, J.R., Trahey, G.E., Nightingale, K.R., and Palmeri, M.L. Acoustic radiation force elasticity imaging in diagnostic ultrasound. IEEE Trans Ultrason Ferroelectr Freq Control **60,** 685, 2013.

41. Chung, C.Y., Heebner, J., Baskaran, H., Welter, J.F., and Mansour, J.M. Ultrasound elastography for estimation of regional strain of multilayered hydrogels and tissue-engineered cartilage. Ann Biomed Eng **43,** 2991, 2015.
42. Greenleaf, J.F., Fatemi, M., and Insana, M. Selected methods for imaging elastic properties of biological tissues. Annu Rev Biomed Eng **5,** 57, 2003.
43. Parker, K.J., Taylor, L.S., Gracewski, S., and Rubens, D.J. A unified view of imaging the elastic properties of tissue. J Acoust Soc Am **117,** 2705, 2005.
44. Palmeri, M.L., and Nightingale, K.R. Acoustic radiation force-based elasticity imaging methods. Interface Focus **1**, 553, 2011.
45. Ophir, J., Cespedes, I., Ponnekanti, H., Yazdi, Y., and Li, X. Elastography: a quantitative method for imaging the elasticity of biological tissues. Ultrason Imaging **13,** 111, 1991.
46. Dewall, R.J. Ultrasound elastography: principles, techniques, and clinical applications. Crit Rev Biomed Eng **41,** 1, 2013.
47. Garra, B.S., Cespedes, E.I., Ophir, J., Spratt, S.R., Zuurbier, R.A., Magnant, C.M., and Pennanen, M.F. Elastography of breast lesions: initial clinical results. Radiology **202,** 79, 1997.
48. Hoeks, A.P.G., Brands, P.J., Willigers, J.M., and Reneman, R.S. Non-invasive measurement of mechanical properties of arteries in health and disease. Proc Inst Mech Eng H **213,** 195, 1999.
49. Kim, K., Jeong, C.G., and Hollister, S.J. Non-invasive monitoring of tissue scaffold degradation using ultrasound elasticity imaging. Acta Biomater **4**, 783, 2008.
50. Lubinski, M.A., Emelianov, S.Y., and O'Donnell, M. Speckle tracking methods for ultrasonic elasticity imaging using short-time correlation. IEEE Trans Ultrason Ferroelectr Freq Control **46,** 82, 1999.
51. Bilgen, M., and Insana, M.F. Deformation models and correlation analysis in elastography. J Acoust Soc Am **99,** 3212, 1996.
52. Nightingale, K., Soo, M.S., Nightingale, R., and Trahey, G. Acoustic radiation force impulse imaging: in vivo demonstration of clinical feasibility. Ultrasound Med Biol **28,** 227, 2002.
53. Nightingale, K.R., Palmeri, M.L., Nightingale, R.W., and Trahey, G.E. On the feasibility of remote palpation using acoustic radiation force. J Acoust Soc Am **110,** 625, 2001.
54. Fahey, B.J., Nightingale, K.R., Stutz, D.L., and Trahey, G.E. Acoustic radiation force impulse imaging of thermally- and chemically-induced lesions in soft tissues: preliminary ex vivo results. Ultrasound Med Biol **30,** 321, 2004.
55. Pinto, J.G., Price, J.M., Fung, Y.C., and Mead, E.H. A device for testing mechanical properties of biological materials—the ''Biodyne''. J Appl Physiol **39,** 863, 1975.
56. Viola, F., Kramer, M.D., Lawrence, M.B., Oberhauser, J.P., and Walker, W.F. Sonorheometry: a noncontact method for the dynamic assessment of thrombosis. Ann Biomed Eng **32,** 696, 2004.
57. Walker, W.F., Fernandez, F.J., and Negron, L.A. A method of imaging viscoelastic parameters with acoustic radiation force. Phys Med Biol **45,** 1437, 2000.
58. Mauldin, F.W., Jr., Haider, M.A., Loboa, E.G., Behler, R.H., Euliss, L.E., Pfeiler, T.W., and Gallippi, C.M. Monitored steady-state excitation and recovery (MSSER) radiation force imaging using viscoelastic models. IEEE Trans Ultrason Ferroelectr Freq Control **55,** 1597, 2008.
59. Gudur, M.S.R., Kumon, R.E., Zhou, Y., and Deng, C.X. High-frequency rapid B-mode ultrasound imaging for real-time monitoring of lesion formation and gas body activity during high-intensity focused ultrasound ablation. IEEE Trans Ultrason Ferroelectr Freq Control **59,** 1687, 2012.
60. Chen, H., Shi, H., and Varghese, T. Improvement of elastographic displacement estimation using a two-step cross-correlation method. Ultrasound Med Biol **33,** 48, 2007.
61. Berglund, J.D., Nerem, R.M., and Sambanis, A. Viscoelastic testing methodologies for tissue engineered blood vessels. J Biomech Eng **127,** 1176, 2005.
62. Rowe, S.L., and Stegemann, J.P. Microstructure and mechanics of collagen-fibrin matrices polymerized using ancrod snake venom enzyme. J Biomech Eng **131,** 061012, 2009.
63. Drury, J.L., Dennis, R.G., and Mooney, D.J. The tensile properties of alginate hydrogels. Biomaterials **25,** 3187, 2004.
64. Svensson, A., Nicklasson, E., Harrah, T., Panilaitis, B., Kaplan, D.L., Brittberg, M., and Gatenholm, P. Bacterial cellulose as a potential scaffold for tissue engineering of cartilage. Biomaterials **26,** 419, 2005.
65. Roach, M., 3rd, Alberini, J.L., Pecking, A.P., Testori, A., Verrecchia, F., Soteldo, J., Ganswindt, U., Joyal, J.L., Babich, J.W., Witte, R.S., Unger, E., and Gottlieb, R. Diagnostic and therapeutic imaging for cancer: therapeutic considerations and future directions. J Surg Oncol **103,** 587, 2011.
66. Urheim, S., Edvardsen, T., Torp, H., Angelsen, B., and Smiseth, O.A. Myocardial strain by doppler echocardiography: validation of a new method to quantify regional myocardial function. Circulation **102,** 1158, 2000.
67. D'Hooge, J., Konofagou, E., Jamal, F., Heimdal, A., Barrios, L., Bijnens, B., Thoen, J., Van de Werf, F., Sutherland, G., and Suetens, P. Two-dimensional ultrasonic strain rate measurement of the human heart in vivo. IEEE Trans Ultrason Ferroelectr Freq Control **49,** 281, 2002.
68. Jia, C., Olafsson, R., Kim, K., Kolias, T.J., Rubin, J.M., Weitzel, W.F., Witte, R.S., Huang, S.W., Richards, M.S., Deng, C.X., and O'Donnell, M. Two-dimensional strain imaging of controlled rabbit hearts. Ultrasound Med Biol **35,** 1488, 2009.
69. Hsu, S.J., Bouchard, R.R., Dumont, D.M., Wolf, P.D., and Trahey, G.E. In vivo assessment of myocardial stiffness with acoustic radiation force impulse imaging. Ultrasound Med Biol **33,** 1706, 2007.
70. Zhai, L., Polascik, T.J., Foo, W.C., Rosenzweig, S., Palmeri, M.L., Madden, J., and Nightingale, K.R. Acoustic radiation force impulse imaging of human prostates: initial in vivo demonstration. Ultrasound Med Biol **38,** 50, 2012.

Address correspondence to:
Cheri X. Deng, PhD
Department of Biomedical Engineering
University of Michigan
Ann Arbor, MI 48109

E-mail: cxdeng@umich.edu

Jan P. Stegemann, PhD
Department of Biomedical Engineering
University of Michigan
Ann Arbor, MI 48109

E-mail: jpsteg@umich.edu

Received: October 5, 2015
Accepted: January 14, 2016
Online Publication Date: February 25, 2016

This article has been cited by:

1. Tingting Xia, Wanqian Liu, Li Yang. 2017. A review of gradient stiffness hydrogels used in tissue engineering and regenerative medicine. *Journal of Biomedical Materials Research Part A* **105**:6, 1799-1812. [CrossRef]
2. Hyun Koo, Kenneth M Yamada. 2016. Dynamic cell–matrix interactions modulate microbial biofilm and tissue 3D microenvironments. *Current Opinion in Cell Biology* **42**, 102-112. [CrossRef]
3. Xiaowei Hong, Jan P. Stegemann, Cheri X. Deng. 2016. Microscale characterization of the viscoelastic properties of hydrogel biomaterials using dual-mode ultrasound elastography. *Biomaterials* **88**, 12-24. [CrossRef]